Resonant multielectron transfer in solid oxides following double K-shell ionization by heavy-ion impact

B. B. Bandong and R. L. Watson

Cyclotron Institute and Department of Chemistry, Texas A&M University, College Station, Texas 77843

(Received 1 September 1988)

The $K\alpha$ hypersatellite spectra of oxygen, obtained by bombardment of various solid oxides with 2-MeV/amu beams of C and Ar ions, were measured using a curved-crystal spectrometer. In the spectra for the compounds CaO, SrO, CeO_2, and three of the oxides of Ti, some of the hypersatellite peaks appeared to be enhanced while others were suppressed. These features are indicative of resonant electron transfer processes caused by the energy matching of valence levels in the multiply ionized oxygen ion with those of its neighboring metal ions. In all cases except CaO, the spectra suggest that correlated multielectron transfer is involved, in which as many as four electrons are exchanged between the two ions. A method developed previously for estimating the energy change associated with the electron exchange was generalized to cover multielectron transfer, and corrections for extra-atomic relaxation were included. Calculations employing this method strongly support the resonant multielectron transfer hypothesis.

I. INTRODUCTION

Outer-shell vacancies created in a chemically bound, low- to intermediate-Z target atom during a K-shell ionizing collision may be filled by the rapid transfer of electrons from neighboring atoms prior to K x-ray emission. Interatomic electron transfer can considerably alter the valence-electron distribution, leading to significant variations in the x-ray satellite intensity distribution from compound to compound.[1,2] Systematic investigations of the fluorine K x-ray spectra of alkali-metal and alkaline-earth fluorides excited with 2-MeV/amu beams of He, C, Mg, and Ar ions have delineated two possible mechanisms for F L-vacancy filling arising from the matching of energy levels between the multiply ionized F atom and the surrounding atoms.[3-6]

In one level-matching scheme, the normally unbound Rydberg levels ($n \geq 3$) of an F ion descend in energy, following single K- plus multiple L-shell ionization by projectile impact, and approach the valence levels of the neighboring metal ions. If the interior potential barrier between fluorine and the metal is small, electrons are free to transfer from the metal ion to the M and N shells of the fluorine ion.[5,6] Subsequent transitions of the transferred electrons to the L shell, prior to K x-ray emission, shift the satellite emission strength toward the lower-order peaks.

Hartmann has recently employed the $X\alpha-$ scattered-wave (SW) method in modeling multiply ionized F atoms in their solid-state environment by choosing octahedral $(FX_6)^{n+}$ and tetrahedral $(FX_4)^{m+}$ next-neighbor cluster units.[7] His calculations on transfer rates and spectral simulations agree reasonably well with the measurements of Benka and co-workers.[4-6] In addition, this author had concluded that, since the availability of overlapping occupied valence states is the only requirement for filling the F ion Rydberg levels, this two-step mechanism for L-vacancy quenching is of a universal (nondiscriminating) nature.

A second mechanism involves a highly efficient, highly selective quenching of F L vacancies by electron transfer proceeding in a single step and leads to significant enhancement (or suppression) of the intensities of specific satellite lines. Deconninck and Van den Brock[8] observed an anomalously low KL^1 satellite ($1s^{-1}2p^{-1}$ initial state) intensity for KF, SrF_2, and BaF_2 in measurements of fluorine spectra excited by α particles. This behavior could not be understood in terms of simple covalency arguments. The same results were obtained by Benka et al.[3] in spectra excited by 5.5-MeV He^+ bombardment of thin targets of alkali-metal and alkaline-earth fluorides. These latter authors proposed a mechanism that involves resonant electron transfer (RET) between the outermost np levels of the metal ion and the $2p$ levels of the fluorine ion. Calculations of the energy-level-matching condition for these cases employing a point-charge model supported the RET explanation. Further evidence of RET has also been found in fluorine K Auger spectra of various fluorides excited by Al $K\alpha$ x-rays.[9]

It is of interest to investigate other systems that might exhibit similar RET phenomena to obtain more information about the process. Studies of ion-excited K x-ray spectra of sodium in solid compounds failed to uncover any evidence for RET to the L shell.[10] Valjakka et al.[11] observed variations in the oxygen KL^1 satellite structure of various ionic solid oxides excited by 4- to 6-keV electrons, but ruled out RET as the cause of the structural dependence. Calculations using the formalism of Benka et al.[3] showed that RET is not energetically favorable for the cases studied.

In the present work, we had initially intended to extend the investigation of chemical effects in oxygen $K\alpha$ x-ray spectra to higher-order satellite lines. However, distortions of the $K\alpha$ satellite spectra due to the O K-

absorption edge, the inherent reflectivity discontinuity of phthalate-containing analyzing crystals used in this spectral region, and the interfering presence of molecular-orbital x-rays in the KL^0–KL^3 region prevented a definitive study. Instead, we have focused our attention on the double-K-vacancy $K\alpha$ hypersatellite region where moderately good spectral resolution and the absence of experimental distortions allowed a detailed examination of the x-ray structure. These measurements have provided evidence for resonant multielectron transfer (RMET) from metal-ion valence shells to the L shell of oxygen ions bearing two K vacancies. The plausibility of this interpretation is demonstrated by application of a formalism, originally developed by Benka et al.[3] that has been modified to include multielectron transfer and extra-atomic relaxation.

II. EXPERIMENTAL METHODS

Beams of 2-MeV/amu C^{2+} and Ar^{5+} ions were extracted from the Texas A&M Variable Energy Cyclotron and directed onto metal oxide targets through a 3-mm-diam collimator located 1 cm in front of the target. The targets were thick pellets of alkali-metal and alkaline-earth oxides, and oxides of Al, Si, Ti(II), Ti(III), Ti(IV), and Ce(IV), made by compacting the powdered compound with a hydraulic press. The Na_2O and K_2O targets were prepared by exposing freshly cut surfaces of the pure metals to air. The purity of the other compounds used was better than 99.9%.

X-rays emitted from the targets were analyzed using a 12.7-cm Johansson-type curved-crystal spectrometer oriented such that the Rowland circle was perpendicular to the ion beam axis. Oxygen K x rays were diffracted with a thallium acid phthalate (TAP, $2d = 25.750$ Å) crystal into a flow-proportional counter that was operated at 1 atm of P-10 gas (90% Ar, 10% CH_4) enclosed by a 65-$\mu g/cm^2$-thick polypropylene window. A resolution of 2 eV was obtained for the hydrogenlike oxygen K^2L^7 ($2p\ ^2P$–$1s\ ^2S$) transition (653.5 eV) excited in an O_2 gas target, measured in the same configuration as the solid oxides. X rays were counted for a given unit of beam charge collected by a thin (10 $\mu g/cm^2$) carbon foil located between the collimator and the target, and the data were stored in a DEC VAX11/780 computer via a computer-aided-measurement-and-control (CAMAC) interface for later analysis.

Identification of the oxygen $K\alpha$ hypersatellites was established by comparing the experimental peak energies with those determined in a previous study of gaseous oxygen targets[12] and with results of Dirac-Fock calculations. Energy calibration of the spectrometer was performed using the $K\alpha_{1,2}$ lines of F (in first order) and the Na $K\alpha_{1,2}$, $K\alpha_3$, $K\alpha_5$, and $K\alpha_9$ lines (in second order) excited in a solid NaF target.

III. RESULTS

The $K\alpha$ hypersatellite spectra of oxygen, obtained by bombarding thick pellets of K_2O, BeO, CaO, SrO, and CeO_2 with carbon ions, are shown in Fig. 1. (Hereafter,

the oxygen $K\alpha$ hypersatellite spectrum for a particular sample such as K_2O will be referred to as "the K_2O spectrum.") The peaks are labeled according to the number of L vacancies, n, in addition to the two K-shell vacancies (i.e., the initial vacancy configuration is specified by the notation K^2L^n where n is the number of L vacancies relative to an O^{2-} ground-state configuration of $1s^22s^22p^6$). The spectrum of K_2O displays a rather symmetric intensity distribution centered between K^2L^2 and K^2L^3. In fact, as is depicted in the bar graph of Fig. 2(a), its relative intensity distribution agrees rather well with a binomial distribution calculated using the experimental p_L value of 0.33, extracted from the spectrum by means of the following equation:

$$p_L = \bar{n}/8 = \frac{1}{8}\sum_{n=0}^{7} nf_n \ , \tag{1}$$

where p_L is the average L-vacancy fraction, n is the number of L-shell vacancies, and f_n is the intensity of the
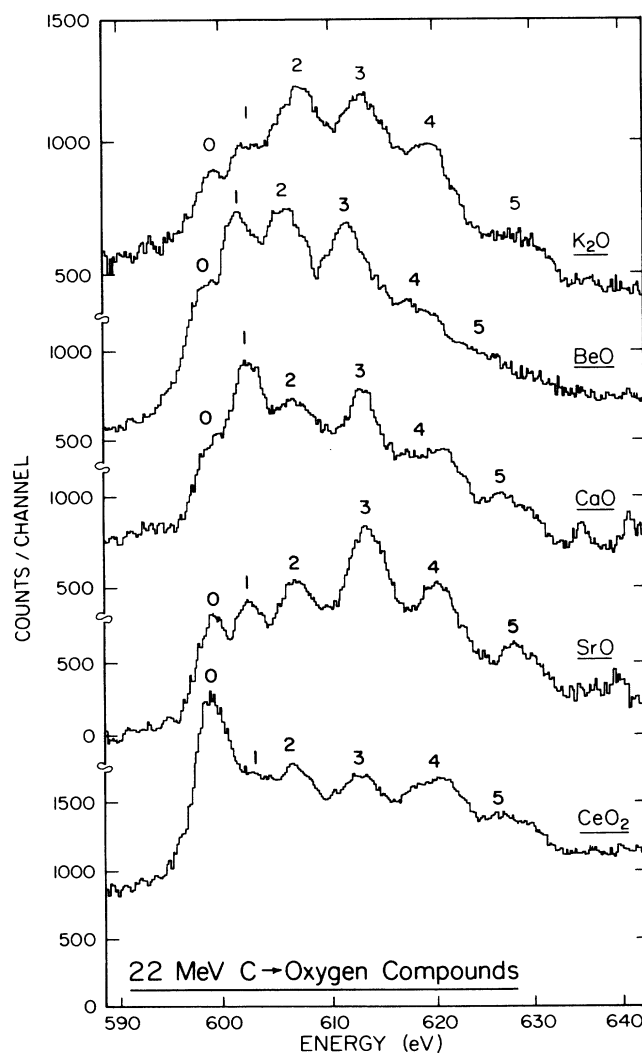
FIG. 1. $K\alpha$ hypersatellite spectra of oxygen in different oxides excited by 22-MeV C ions.
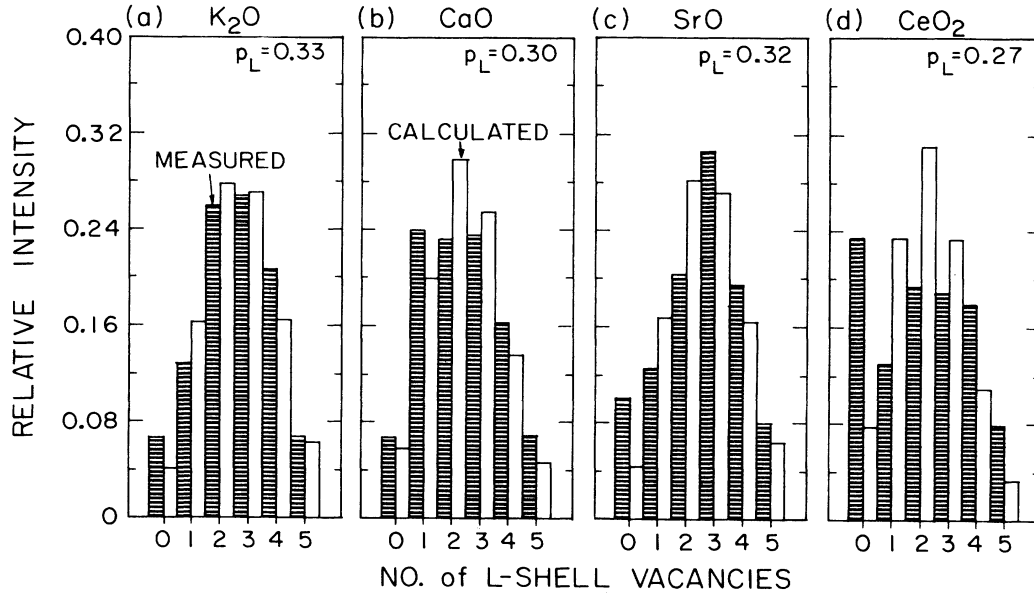
FIG. 2. Comparison of the oxygen $K\alpha$ hypersatellite relative intensities with binomial distributions for K_2O, CaO, SrO, and CeO_2 excited by 22-MeV ions.

K^2L^n hypersatellite peak relative to the total intensity. The shift of the intensity distribution towards the lower-order hypersatellite peaks in the spectrum (Fig. 1) of the more covalent BeO ($p_L = 0.29$) is consistent with a two-step rapid electron transfer mechanism whereby the Rydberg levels ($3s$ $3p$, $3d$) of oxygen, following a collision in which two K plus n L electrons are removed, descend and become matched in energy with the valence levels of neighboring ions.[7] This level-matching condition leads to the population of M-shell levels in the multiply ionized oxygen ion. The oxygen M electrons then undergo LMM Auger transitions, thus filling L vacancies and shifting the K x-ray emission strength toward the lower-order hypersatellites. In BeO, neighboring Be^{2+} cations do not provide donor valence states, but other O^{2-} ions are sufficiently close to the x-ray-emitting O ion that their valence levels can provide the electrons instead. As in the case of K_2O, the hypersatellite intensity distribution of BeO is reasonably well represented by a binomial distribution.

That rapid electron transfer is quite extensive in BeO is further evidenced by the shifts to lower energies of the hypersatellite peaks in the BeO spectrum relative to corresponding peaks in the spectra of the more ionic oxides K_2O, CaO, SrO, and CeO_2 (see Fig. 1). The most likely cause of the observed downward energy shifts is screening caused by the presence of several electrons in outer ($n \geq 3$) energy levels of the oxygen ion. These electrons are presumably transferred from the valence states of near-neighbor oxygen ions prior to K x-ray decay.

An examination of the CaO spectrum in Fig. 1 reveals that the K^2L^1 peak intensity is greatly enhanced and the K^2L^2 peak intensity is suppressed relative to the K_2O spectrum. Likewise, for SrO the K^2L^2 peak is also suppressed in intensity; however, it is the K^2L^0 peak that appears to have gained intensity while the K^2L^1 peak

remains unaffected. In CeO_2, the K^2L^0 peak is greatly enhanced relative to the other hypersatellite peaks. To ensure that no interfering Ce x-ray lines (in particular, M and N x-rays) lie in this energy region, the spectra of CeF_4 and $CeCl_4$ targets were also measured. No lines were seen in the region of the oxygen hypersatellites. The bar graphs in Fig. 2 also show that the K^2L^1 peak of CaO and the K^2L^0 peaks of SrO and CeO_2 are enhanced relative to the binomial intensities, while the relative intensities of K^2L^2 in CaO and SrO, and of the K^2L^1 and K^2L^2 peaks in CeO_2 are suppressed.

Assuming the peculiar behavior described above for CaO, SrO, and CeO_2 is caused by resonant electron transfer, then the following electron transfer reactions are likely candidates: for CaO,

$$Ca^{2+}(g.s.) + O^{2+}(1s^{-2}2p^{-2})|_{(K^2L^2)}$$

$$= Ca^{3+}(3p^{-1}) + O^+(1s^{-2}2p^{-1})|_{(K^2L^1)}, \quad (2a)$$

for SrO,

$$Sr^{2+}(g.s.) = O^{2+}(1s^{-2}2p^{-2})|_{(K^2L^2)}$$

$$= Sr^{4+}(4p^{-2}) + O^0(1s^{-2})|_{(K^2L^0)}, \quad (2b)$$

for CeO_2,

$$Ce^{4+}(g.s.) + O^+(1s^{-2}2p^{-1})|_{(K^2L^1)}$$

$$= Ce^{5+}(5p^{-1}) + O^0(1s^{-2})|_{(K^2L^0)}, \quad (2c)$$

and/or,

$$Ce^{4+}(g.s.) + O^{2+}(1s^{-2}2p^{-2})|_{(K^2L^2)}$$

$$= Ce^{6+}(5p^{-2}) + O^0(1s^{-2})|_{(K^2L^0)}. \quad (2d)$$
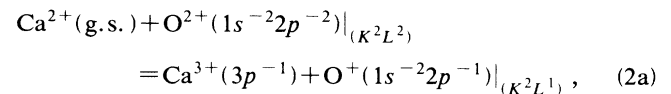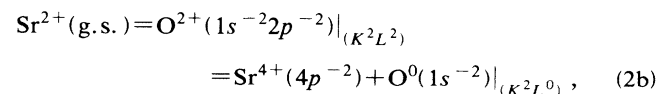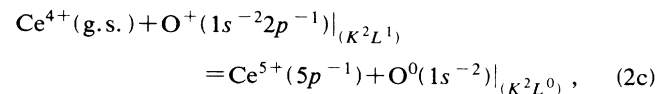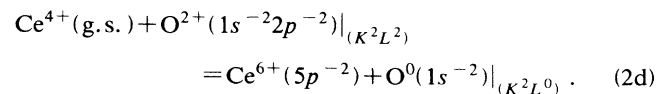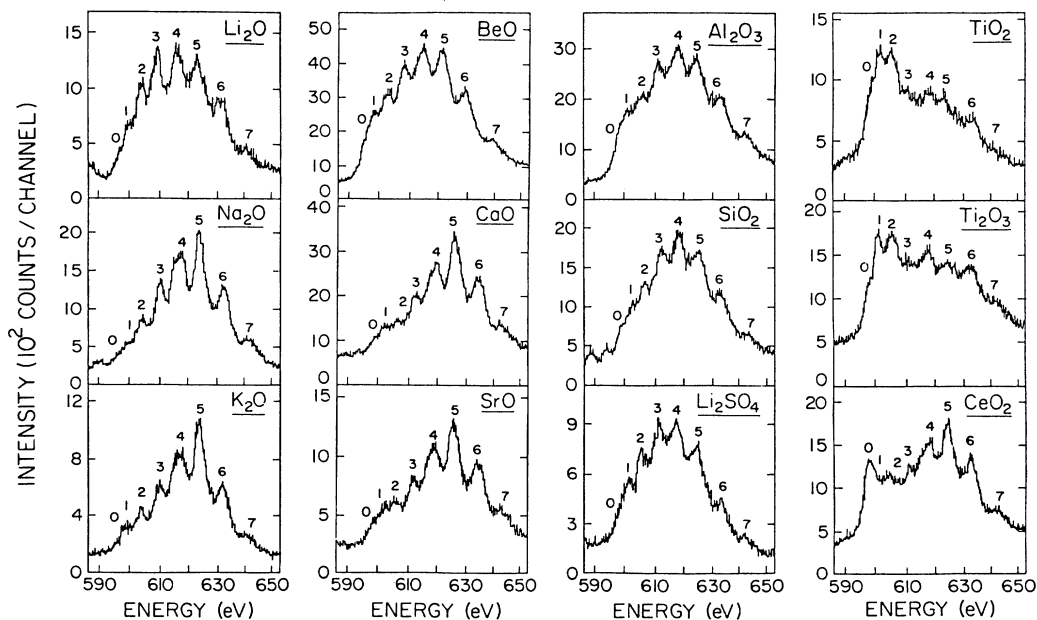
FIG. 3. Oxygen $K\alpha$ hypersatellite spectra of a variety of metal oxides excited by 80-MeV Ar ions.

Reactions (2a) and (2c) involve one-electron transfer from the metal outer np levels to the oxygen $2p$ levels, while reactions (2b) and (2d) involve correlated two-electron (electron-pair) transfer. Taking the case of CaO as an example, $O^{2+}(1s^{-2}2p^{-2})$ represents a collision-excited oxygen ion having an electron configuration of $2s^2 2p^4$, Ca^{2+} (g.s.) represents a nearest-neighbor Ca metal ion in its electronic ground state (outer-shell configuration of $3s^2 3p^6$), $Ca^{3+}(3p^{-1})$ represents the metal ion with a $3p$ electron removed, and $O^+(1s^{-2}2p^{-1})$ represents an oxygen ion with two $1s$ vacancies and a single $2p$ vacancy. Presumably when the energy change ΔE associated with this process is zero, an electron is free to transfer between the two ions if the barrier penetration probability is high (i.e., if the Coulomb barrier between the two ions is small). The effect of this resonance on the observed $K\alpha$ x-ray hypersatellite spectrum would be to transfer intensity from the K^2L^2 or K^2L^1 peaks to the K^2L^1 or K^2L^0 peaks for the single-electron transfer cases (2a) and (2c), and from the K^2L^2 peak to the K^2L^0 peak for the electron-pair transfer cases (2b) and (2d).

The Ar-excited $K\alpha$ hypersatellite spectra of some of the oxides are shown in Fig. 3. For similar projectile velocities, excitation by Ar ions produces higher stages of ionization, on average, than excitation by C ions, as is indicated by the shift of the relative intensity distribution towards the higher-order hypersatellites. In fact, the experimental p_L values increase from about $0.30-0.35$ with C excitation to $0.50-0.55$ with Ar excitation for these oxides. It can also be seen that the most covalent oxides, such as Li_2O, BeO, Al_2O_3, SiO_2, and Li_2SO_4, display intensity distributions that are nearly symmetric about the K^2L^4 peak. On the other hand, the more ionic oxides (Na_2O, K_2O, CaO, and SrO) show distributions that are skewed toward the high-n hypersatellite peaks. Of par-

ticular interest are the spectra of the titanium oxides which show anomalously enhanced peak intensities for K^2L^1 and K^2L^2. The absence of interfering Ti L and M x rays was confirmed by taking the spectra of Ti metal and $TiCl_2$ using 5-keV electron excitation. No lines were observed in this region.

In view of the fact that the proposed electron transfer mechanisms are expected to be independent of the mode of excitation, it is noteworthy that the Ar-excited spectrum of CeO_2 displays a highly enhanced K^2L^0 peak similar to that observed with C excitation. On the other hand, although the Ar-excited spectra of CaO and SrO show enhanced peak intensities for K^2L^1 and K^2L^0, respectively, and suppressed K^2L^2 peak intensities when compared to the spectra for Na_2O and K_2O, these features do not show up as clearly as they do in the C-excited spectra. In addition to the fact that relatively fewer of the low-n hypersatellite states are produced with Ar excitation than with C excitation, only one RET process is operative for CaO [reaction (2a)] and SrO [reaction (2b)], while in CeO_2 two RET processes are possible [reactions (2c) and 2(d)].

IV. ANALYSIS AND DISCUSSION

A. Formulation of the resonance condition

In order to demonstrate the plausibility of the preceding arguments concerning RET and RMET, it is necessary to devise a method for calculating the energy change associated with electron transfer, ΔE. Presented here is a method based on the procedure developed by Benka et al.[3] for the alkali-metal and alkaline-earth fluorides. It has been generalized to cover multielectron transfer and corrections for extra-atomic relaxation (polarization)

have been included.

Consider the general case of a crystal lattice $A_j B_i$ where j and i are the relative numbers of atoms which exist in the crystal as ions A^{i+} and B^{j-}. After an ionizing collision by a projectile, the ions are left with charges A^{i+m} and B^{-j+n}; that is, m electrons are removed from A^{i+} and n electrons from B^{j-}. The transfer of q electrons from A to B may be represented by

$$A^{i+m} + B^{-j+n} = A^{(i+m)+q} + B^{(-j+n)-q} . \tag{3}$$
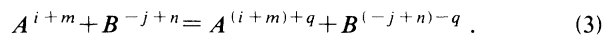
The energy change for the q-electron transfer process represented by reaction (3) may be expressed as the sum of (a) the energy expended to remove q electrons (to infinity) from the outer levels of a metal ion located adjacent to a B^{-j+n} ion, and (b) the energy released when q electrons are brought (from infinity) to some energy level of the B^{-j+n} ion. The energy for (b) is equal, but opposite in sign, to the energy required for the inverse process of removing q electrons from the ion $B^{(-j+n)-q}$ located next to an $A^{(i+m)+q}$ ion. Hence the energy change ΔE can be calculated by taking the difference of the binding energy of q electrons from the ion A^{i+m} and the binding energy of q electrons from the ion $B^{(-j+n)-k}$, and accounting for the crystal lattice environment.

Using Mahan's localized-hole point-ion (LHPI) model,[13,14] the energy required to remove q electrons from an ion in a crystal lattice is

$$E_b(qe) = E_{IP}^0(qe) \pm qE_M + E_C - E_{rx}(q) , \tag{4}$$

where $E_{IP}^0(qe)$ is the free-ion ionization energy for q electrons and E_M is the Madelung energy arising from the electrostatic interaction of an electron with the other ions of the lattice. The $+qE_M$ term applies for the anion B and the $-qE_M$ term applies for the cation A. The Madelung energy E_M is the Madelung constant M_c multiplied by ze^2/r_0, where r_0 is the nearest-neighbor distance and z is the greatest common factor between the cation and anion ground-state charges. (For example, in $A_2 B_4$ the charge of A is $4+$, which factors as 1×4 and 2×2, while the charge of B is $2+$, which factors as 1×2, and hence for this case $z = 2$.) The Coulomb energy E_C is the additional electrostatic energy arising from the extra charges on the ions A and B over and above those which are accounted for by the Madelung energy term.

The last term $E_{rx}(q)$ is the extra-atomic relaxation energy (polarization energy) for the removal of q electrons from an ion in the lattice. Mahan[13,14] has identified two components contributing to the extra-atomic relaxation energy: the traditional Mott-Littleton energy Σ_{ML} and an additional hole self-energy Σ_2. The calculations of Mahan[13] have shown that the magnitude of Σ_{ML} is independent of the hole site and that it varies quadratically with the change in charge of the ion. They also demonstrated that inclusion of the Σ_2 term in the calculation of the absolute binding energy of an electron to an ion in a crystal leads to a considerable improvement when compared with experiment. Physically, Σ_2 represents a screening of the Madelung potential in the presence of a core hole. Like Σ_{ML}, its magnitude is independent of the core hole site, but unlike Σ_{ML}, it varies linearly with the

change in charge. For systems of high symmetry, such as the alkali-metal halides (NaCl structure), it has been shown by Matthew et al.[15] that the Σ_2 value is the same for both alkali-metal cation and halide anion, and hence cancels in the calculation of binding energy differences. This is probably the reason why previous investigators (Citrin and Thomas[16] and Poole et al.[17]) have overlooked this term. In the succeeding numerical calculations of ΔE, the Σ_2 contribution is totally neglected since only differences in the binding energies of the cation and anion are required. However, for completeness, the Σ_2 factor will be included in the following formulation.

A matter of importance in the present application concerns the fact that all of the reported procedures for calculating Σ_{ML} and Σ_2 are for cases involving single ionization of an ion in its ground-state configuration. Here, however, we are dealing with multiply ionized atoms, and hence it was necessary to correct the single ionization values of Σ_{ML} and Σ_2 using a scaling procedure. As previously indicated, Σ_{ML} varies quadratically and Σ_2 linearly with the change in charge, so that the total relaxation energy for q-electron ionization of an ion may be written as

$$E_{rx}(q) = q^2 \Sigma_{ML} + q \Sigma_2 . \tag{5}$$

As an example of the application of Eq. (5), consider the case represented by reaction (2a), in which an electron is transferred from the $3p$ level of Ca^{2+} to the $2p$ level of an O^{2+} ion having a $2s^2 2p^4$ electron configuration. For the purpose of calculating the oxygen ion relaxation energy, it is convenient to focus on the inverse process (i.e., ionization) represented by

$$O^+(1s^{-2} 2p^{-1})\big|_{(K^2 L^1)} = O^{2+}(1s^{-2} 2p^{-2})\big|_{(K^2 L^2)} + e^- . \tag{6}$$
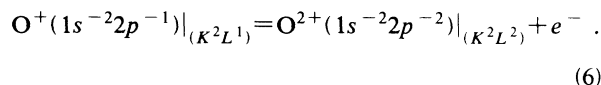
Reaction (6) can be expressed as the difference of two ionization reactions involving the ground state $O^{2-}(1s^2 2s^2 2p^6)$:

$$O^{2-}(1s^2 2s^2 2p^6) = O^{2+}(2s^2 2p^4) + 4e^- , \tag{6a}$$

$$O^{2-}(1s^2 2s^2 2p^6) = O^+(2s^2 2p^5) + 3e^- . \tag{6b}$$

Under the assumption that the magnitude of the relaxation energy is independent of the hole site, the relaxation energies for reactions (6a) and (6b) are, respectively,

$$E_{rx}(O^{2-}, 4e) = 16 \Sigma_{ML} + 4 \Sigma_2 , \tag{7a}$$

$$E_{rx}(O^{2-}, 3e) = 9 \Sigma_{ML} + 3 \Sigma_2 . \tag{7b}$$

Thus the total relaxation energy for reaction (6) is

$$E_{rx}(O^+ \to O^{2+}, 1e) = E_{rx}(O^{2-}, 4e) - E_{rx}(O^{2-}, 3e)$$

$$= 7 \Sigma_{ML} + \Sigma_2 . \tag{8}$$

The same arguments hold for the cation.

From the above discussion, it follows that the energy change for the q-electron transfer process represented by reaction (3) is given by

$$\Delta E = [E^0_{IP}(A^{i+m}, qe) - E^0_{IP}(B^{-j+n-q}, qe)]$$
$$- q[E_M(A) + E_M(B)] + [E_C(A) - E_C(B)]$$
$$- [E_{rx}(A, qe) - E_{rx}(B, qe)] . \tag{9}$$

The first term in brackets is the difference in the total q-electron ionization potentials of the free ions A^{i+m} and B^{-j+n-q}. The next two terms in brackets, which involve E_M and E_C, represent the net Coulomb energy contribution to the energy change ΔE. The origin of these terms may be understood by considering reaction (3) for the case of one-electron transfer ($q = 1$), as an example. The electron being removed from the ion A^{i+m} experiences a Coulomb interaction with the rest of the ions in the lattice. This interaction energy is given by $-E_M(A)$. However, because of the extra charge on the adjacent B^{-j+n} ion, the electron experiences an additional Coulomb energy change $E_C(A)$ of ne^2/r_0. When this same electron is added to the B^{-j+n} ion, it experiences an energy change $E_M(B)$ due to the Coulomb interaction with the other ions in the lattice, and, because of the extra charge on the adjacent ion (which is now $A^{(i+m)+1}$), there is an additional Coulomb energy change $E_C(B)$ of $-(m+1)e^2/r_0$. In general, the net Coulomb energy change for the transfer of q electrons is

$$E_{C, net} = -q[E_M(A) + E_M(B)] + [E_C(A) - E_C(B)]$$
$$= -2qze^2[M_c(A_j B_i)]/r_0 + q(n - m - q)e^2/r_0 , \tag{10}$$

where, in the final expression, the Madelung constant $M_c(A_j B_i)$ has been introduced instead of using the Madelung energy E_M, in order to avoid possible confusion caused by the existence of different definitions of E_M.[18]

Finally, the last term in brackets in Eq. (9) expresses the net extra-atomic relaxation energy associated with the electron transfer. From the properties of Σ_{ML} and Σ_2, it follows that the net relaxation energy may be expressed by

$$E_{rx, net} = -[E_{rx}(A) - E_{rx}(B)]$$
$$= -(q^2 + 2mq)\Sigma_{ML}(A) + (2nq - q^2)\Sigma_{ML}(B)$$
$$- q[\Sigma_2(A) - \Sigma_2(B)] . \tag{11}$$

Thus Eq. (9) for the energy change in the q-electron transfer process represented by reaction (3) reduces to the more useful form

$$\Delta E = [E^0_{IP}(A^{i+m}, qe) - E^0_{IP}(B^{-j+n-q}, qe)]$$
$$- 2qze^2[M_c(A_x B_y)]/r_0 + q(n - m - q)e^2/r_0$$
$$- (q^2 + 2mq)\Sigma_{ML}(A) + (2nq - q^2)\Sigma_{ML}(B)$$
$$- q[\Sigma_2(A) - \Sigma_2(B)] . \tag{12}$$

B. Calculations for CaO, SrO, and CeO$_2$

The only calculations of Σ_{ML} that have been reported in the literature[13,14] are for alkali-metal halide and alkaline-earth chalcogenide compounds belonging to the highly symmetric NaCl crystal structure. These values have been used in the present estimates of ΔE for the alkali-metal fluorides and alkaline-earth oxides. Values of Σ_{ML} for CeO$_2$, which has the fluorite structure, were estimated in two ways: (a) by applying corrections for the differences in charge and lattice constant to Mahan's values for BaO, and (b) by employing the method of Mott and Littleton.[19] The former method yielded 4.03 and 2.53 eV for Ce^{4+} and O^{2-}, respectively, while the latter method gave 3.83 and 2.71 eV. The averages of the above values were used in the calculations for CeO$_2$.

TABLE I. Calculated energy change ΔE for one-electron transfer to the K^2L^2 state of oxygen in alkaline-earth oxides and to the KL^1 state of fluorine in alkali-metal fluorides. The values for Σ_2 and Σ_{ML} were taken from Mahan (Refs. 13 and 14). (All quantities are in eV.)

Alkaline-earth oxides: $M^{2+}(g.s.) + O^{2+}(1s^{-2}2p^{-2}) = M^{3+}(np^{-1}) + O^+(1s^{-2}2p^{-1})$

| | | | | ΔE | |
| | | | | without | with |
$M^{2+}(np)$	Σ_2	$\Sigma_{ML}(O^{2-})$	$\Sigma_{ML}(M^{2+})$	E_{rx}	E_{rx}
Mg$^{2+}(2p)$	4.954	2.483	4.057	10.3	23.6
Ca$^{2+}(3p)$	2.673	2.603	3.496	−15.3	−0.5
Sr$^{2+}(4p)$	1.481	2.556	3.055	−20.4	−5.5
Ba$^{2+}(5p)$	0.460	2.599	2.756	−25.2	−9.8

Alkaline-metal fluorides: $M^+(g.s.) + F^+(1s^{-1}2p^{-1}) = M^{2+}(np^{-1}) + F^0(1s^{-1})$

| | | | | ΔE | |
| | | | | without[a] | with |
$M^+(np)$	Σ_2	$\Sigma_{ML}(F^-)$	$\Sigma_{ML}(M^+)$	E_{rx}	E_{rx}
Na$^+(2p)$	1.168	1.480	2.167	11.3	13.6
K$^+(3p)$	0.064	1.693	1.731	−2.1	1.1
Rb$^+(4p)$	−0.254	1.796	1.641	−5.7	−2.0
Cs$^+(5p)$	−0.961	2.201	1.604	−5.9	−3.3

[a]Taken from Benka et al. (Ref. 3).

A value of Σ_{ML} has not been reported for TiO, even though it belongs to the NaCl crystal lattice group. However, the Σ_{ML} for the cations in alkaline-earth oxides vary monotonically as a function of the cation radius. This behavior follows from the fact that the cation polarizability is not affected by its environment.[20] Using the values reported for the alkaline-earth oxides as a calibration of Σ_{ML} versus cation radius yielded a value of 3.7 eV for Ti^{2+}. An average value of 2.6 eV was used for O^{2-}, since the values of Σ_{ML} for oxygen in the different oxides are within 0.1 eV of each other (Ref. 14).

The results of calculations for single-electron RET to the K^2L^2 state of oxygen in alkaline-earth oxides, employing Eq. (12), are given in Table I. The r_0 values used in these calculations were obtained from Gray[21] and Wyckoff,[22] and a Madelung constant of 1.747 56 was adopted for the NaCl lattice structure.[23] The free-ion ionization potentials of the metals were obtained from tabulations of Moore,[24] while that of oxygen was obtained by taking the difference between Dirac-Fock average-of-configuration energies of initial and final states, calculated using the program of Desclaux.[25] For $O^+(1s^{-2}2p^{-1})$ going to $O^{2+}(1s^{-2}2p^{-2})$, the ionization energy was calculated to be 42.5 eV. It can be seen in Table I that when E_{rx} is included in the calculation of ΔE, the experimental observation is correctly predicted (i.e., $\Delta E \approx 0$ for CaO and only CaO). It is also apparent that E_{rx} makes a significant contribution to ΔE in these cases.

Also presented in Table I is a comparison of the ΔE values calculated for one-electron transfer to the KL^1 state in the alkali-metal fluorides, with and without inclusion of the E_{rx} term. It is reassuring to find that the experimentally observed resonance[3] is predicted for KF in either case. It should be noted, that for the alkali-metal fluorides, the contribution of E_{rx} is at most about 2–3 eV so that Benka et al.[3] were justified in neglecting the polarization energy. In the present study, the rather large polarization energies for the oxides arise from the additional charge associated with the double-K-shell vacancy configuration of oxygen, and because oxygen is less electronegative than fluorine, making it more polarizable.

It was noted in Sec. III that the K^2L^0 peak of SrO is quite enhanced. Although it is believed that the enhancement comes from the K^2L^2 state via a two-electron process, it is worthwhile here to see if one-electron transfer to the K^2L^1 state is a possible contributor. In Table II, ΔE values calculated for one-electron transfer to the K^2L^1 state of oxygen in alkaline-earth oxides are presented. Only in BaO is RET to the K^2L^1 state predicted.

TABLE II. Calculated energy change ΔE (eV) for one-electron transfer to the K^2L^1 state of oxygen in alkaline-earth oxides.

$M^{2+}(g.s.) + O^+(1s^{-2}2p^{-1}) = M^{3+}(np^{-1}) + O^0(1s^{-2})$		
	without	with
$M^{2+}(np)$	E_{rx}	E_{rx}
$Mg^{2+}(2p)$	24.9	33.2
$Ca^{2+}(3p)$	0.2	9.7
$Sr^{2+}(4p)$	−4.6	5.2
$Ba^{2+}(5p)$	−9.0	1.2

TABLE III. Calculated energy (eV) for q-electron transfer, ΔE, from the Sr^{2+}(g.s.) $4p$ level to the $2p$ level of oxygen in various hypersatellite (K^2L^n) states. Numbers in parentheses are ΔE values with E_{rx} neglected.

Initial state of oxygen prior to e transfer	Final state of O after electron transfer		
	K^2L^0	K^2L^1	K^2L^2
K^2L^1	5.17 (−4.55)		
K^2L^2	−1.55 (−20.21)	−5.53 (−20.37)	
K^2L^3	−17.57 (−43.75)	−25.47 (−54.14)	−18.54 (−38.49)
K^2L^4	−46.20 (−79.11)	−57.99 (−99.50)	−55.18 (−94.08)
K^2L^5	−88.79 (−127.43)	−105.50 (−158.88)	−106.61 (−163.46)

Unfortunately, a complete spectrum of BaO could not be obtained because the target decomposed during bombardment, causing large spectral distortions. However, the first part of the spectrum, collected before decomposition had progressed very far, showed strong indications of K^2L^0 enhancement.

The results of calculations for one- to five-electron transfer to K^2L^n states ($n = 0-5$) of oxygen in SrO are presented in Table III. The numbers in parentheses give the ΔE values obtained when the E_{rx} term was neglected. These calculations are estimated to be uncertain at the level of 3 or 4 eV, with 1–2 eV arising from the uncertainty in the ionization potentials of the free ions and about 2 eV from the uncertainty in Σ_{ML}. Thus, for SrO, only two-electron transfer from the Sr $4p$ level to the $2p$ level of oxygen in a K^2L^2 state appears to be energetical-

TABLE IV. Calculated energy (eV) for q-electron transfer, ΔE, from the Ce^{4+}(g.s.) $5p$ level to the $2p$ level of oxygen in various hypersatellite (K^2L^n) states. Numbers in parentheses are ΔE values with E_{rx} neglected.

Initial state of oxygen prior to e transfer	Final state of O after electron transfer		
	K^2L^0	K^2L^1	K^2L^2
K^2L^1	4.09 (−4.51)		
K^2L^2	−2.59 (−16.80)	−6.11 (−19.77)	
K^2L^3	−24.15 (−40.95)	−25.30 (−49.61)	−18.62 (−37.32)
K^2L^4	−61.78 (−78.23)	−63.06 (−95.02)	−54.00 (−88.42)
K^2L^5	−115.63 (−128.67)	−119.08 (−153.21)	−110.16 (−157.28)

ly favorable. This prediction is consistent with the enhanced K^2L^0 peak and the suppressed K^2L^2 peak exhibited by the SrO spectrum (relative to those in the K_2O spectrum) in Fig. 1, and strongly supports the case for resonant two-electron transfer.

The ΔE values for one- to five-electron transfer in CeO_2 are given in Table IV. The uncertainty associated with the calculations for this compound is of the order of 5 eV as a consequence of (a) the added uncertainty in the Σ_{ML} values, and (b) the likelihood that the net Σ_2 is not entirely negligible for the fluorite lattice type. As shown in Table IV, the observed strong enhancement in the peak intensity of the K^2L^0 peak can be accounted for by a two-electron transfer from Ce $5p$ to O K^2L^2 $2p$ ($\Delta E = -2.6$ eV) and/or a one-electron transfer to the O K^2L^1 $2p$ ($\Delta E = 4.1$ eV). Within the uncertainty of the calculation, both processes appear to be possible and may indeed contribute to the observed spectrum in Fig. 1.

C. RMET in titanium oxides

It can be seen from Fig. 3 that the Ar ion excited $K\alpha$ hypersatellite spectra of TiO_2 and Ti_2O_3 are very similar. Moreover, the highly enhanced K^2L^1 and K^2L^2 peaks, and the almost equal intensities of the K^2L^3 to K^2L^6 peaks, are features that are unique to these particular ox-

ides. In Fig. 4 $K\alpha$ hypersatellite spectra are compared according to the crystal lattice structure of the compound. It is shown in Fig. 4(a) that oxides having the same crystal structure and comparable ionicities display nearly identical hypersatellite intensity distributions. The comparison in Fig. 4(b), on the other hand, shows that spectra for oxides belonging to different lattice types display distinctly different features, even if they are of similar polar character, as in the case of the Li_2O-BeO pair. In Fig. 4(c), the hypersatellite spectra of the titanium oxides are compared with spectra of other oxides having the same crystal structure and ionicity. (In the TiO_2-Li_2SO_4 pair, Li_2SO_4 actually has a tetragonal structure, and while TiO_2 has the rutile form, its base structure is also a tetragon.[26]) Instead of displaying similar structure, as was the case for the comparison in Fig. 4(a), these spectra exhibit features that are quite different from each other. Relative to the other spectra for the same lattice types, the titanium oxides show highly enhanced K^2L^1 and K^2L^2 peaks and suppressed K^2L^3, K^2L^4, and K^2L^5 peaks.

The anomalous structure in the spectra of the titanium oxides strongly suggests that RMET is involved. Consider the case of the TiO-CaO pair, for example. Both of these oxides are highly ionic. The corresponding K^2L^3,
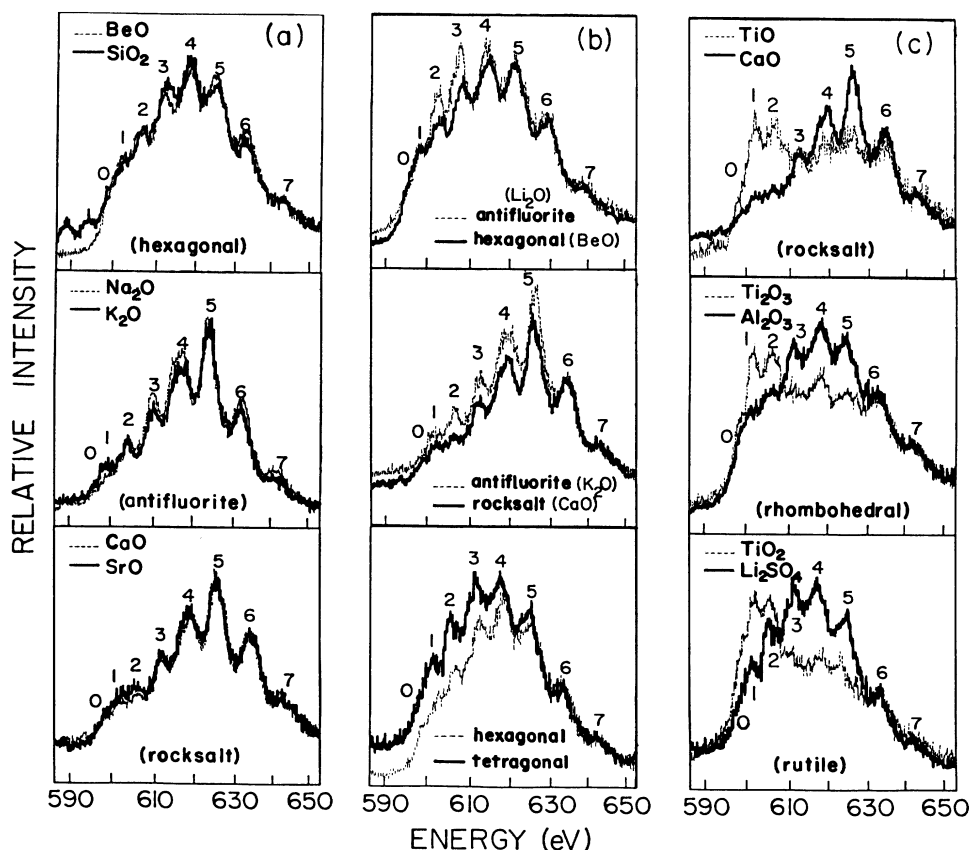
FIG. 4. Comparisons of the hypersatellite structure of oxygen compounds, excited by 80-MeV Ar ions, according to their crystal structures. [The bottom portion of Fig. 4(b) shows spectra of Li_2SO_4 and SiO_2 which have tetragonal and hexagonal lattice types, respectively.]

K^2L^6, and K^2L^7 peaks [labeled 3, 6, and 7, respectively, in Fig. 4(c)] overlap well with each other; however, for TiO the intensities of K^2L^1 and K^2L^2 are much larger and the intensities of K^2L^4 and K^2L^5 are much smaller than the intensities of the corresponding peaks in the CaO spectrum. The following electron transfer processes would explain these features:

two-electron transfer to K^2L^4 enhances K^2L^2 intensity,

three-electron transfer to K^2L^4 enhances K^2L^1 intensity,

three-electron transfer to K^2L^5 enhances K^2L^2 intensity,

four-electron transfer to K^2L^5 enhances K^2L^1 intensity.

The energy change ΔE associated with the transfer of electrons from Ti $3p$ levels to O $2p$ levels was calculated using Eq. (12) for each of the processes

$$\text{Ti}^{2+m}+\text{O}^{-2+n}=\text{Ti}^{(2+m)+q}(3p^{-q})+\text{O}^{(-2+n)-q}, \quad (13)$$
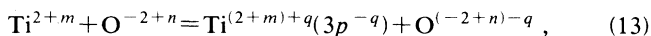
where $m=0-2$ and $n=2-5$. The following parameters were used in the calculations: $\Sigma_{\text{ML}}=3.7$ eV for Ti^{2+} and 2.6 eV for O^{2-}; $r_0=2.088$ Å (Ref. 22). The free-ion ionization energy for the q-electron transfer was calculated for both the $3p$ level of Ti^{2+m} and the $2p$ level of $\text{O}^{(-2+n)-q}$ by taking differences of Dirac-Fock average-of-configurations energies between initial and final states. The calculated ionization energies are estimated to be accurate to within $1-2$ eV.

The results are shown schematically in Fig. 5 for different ionization stages of Ti $(m=0,1,2)$. The ground-state configuration of titanium in the TiO crystal lattice is

$$\text{Ti}^{2+}\ 1s^22s^22p^63s^23p^63d^2 \quad (m=0),$$
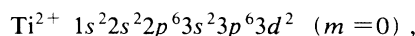
that is, the two outermost $4s$ electrons have been lost in bond formation with oxygen [Fig. 5(a)]. In Ti_2O_3, Ti has a ground-state configuration of $\text{Ti}^{3+}\ 1s^22s^22p^63s^23p^63d^1$ [Fig. 5(b)] and in TiO_2 of $\text{Ti}^{4+}\ 1s^22s^22p^63s^23p^6$ [Fig. 5(c)]. Contributions from Ti^{4+} configurations could conceivably be present in the TiO spectrum since the two $3d$ electrons are loosely bound and hence could be ionized in the collision to give Ti^{4+} $(m=2)$. Also, it is well known that in $3d$ transition-metal compounds, the metal cation can be present in a mixed valence state (i.e., composed of $3d^0$, $3d^1$, and $3d^2$ configurations for Ti).[27] This could be the reason why the spectra of the titanium oxides (Figs. 3 and 4) are so similar, despite the differences in their crystal structures.

The initial and final states of the oxygen ion are represented in Fig. 5 using the K^2L^n convention. The K^2L^n level at $\Delta E=0$ (in the middle of each "level diagram") represents the final state of the oxygen ion after q-electron transfer to the initial $K^2L^{n'}$ state has occurred. In each level diagram, the initial states are positioned to the left and right of the final state and the number of electrons involved in the transfer, q, is written beneath each initial state. Thus in Fig. 5(a), for example, the initial state K^2L^5 connected by a dashed line to the final state

K^2L^0 represents a five-electron transfer. The ΔE for this process is shown to be 16 eV.

Solid lines connecting initial and final states in Fig. 5 (as opposed to dashed lines) represent transitions for which $|\Delta E| \leq 4$ eV. Since the uncertainty in the calculated ΔE values for the titanium oxides is estimated to be of the order 4 eV, these cases represent possible RMET transitions. As indicated in Fig. 5, the following RMET processes appear to be energetically favorable: Ti^{2+},

$K^2L^4 \rightarrow K^2L^1$ (three-electron transfer),

$K^2L^3 \rightarrow K^2L^2$ (one-electron transfer),
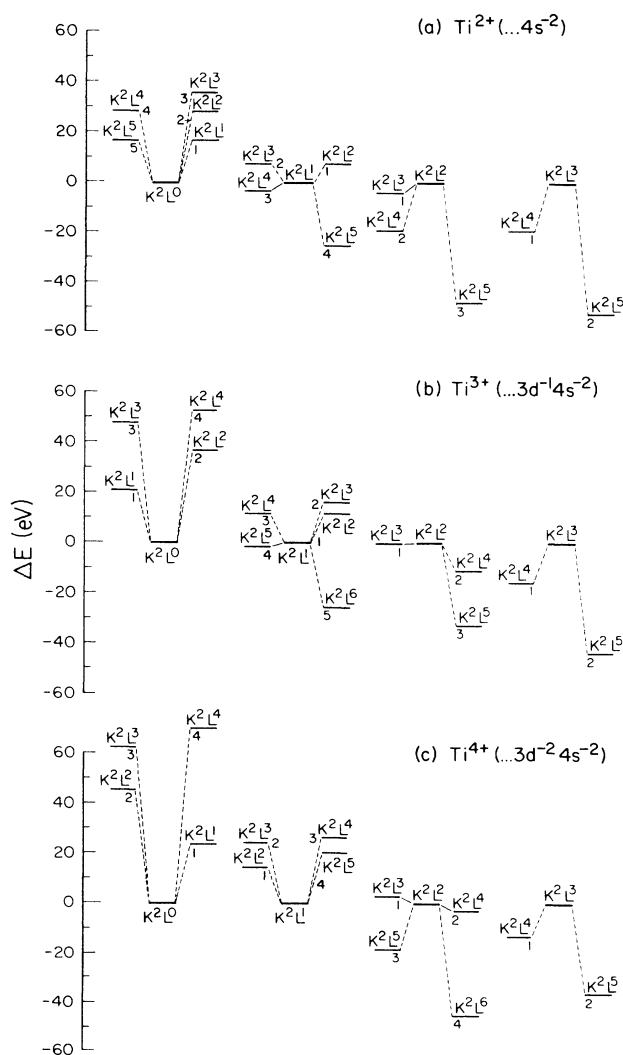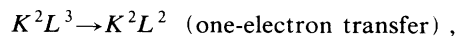
FIG. 5. Schematic representation of the energy associated with electron transfer in titanium oxides. An electron transfer process (shown by a dashed or solid line) changes the initial-state configuration of the oxygen ion from that labeled by the level on the right or left to the final-state configuration labeled by the level in the center. Further details are given in the text.

Ti^{3+},

$K^2L^5 \rightarrow K^2L^1$ (four-electron transfer) ,

$K^2L^3 \rightarrow K^2L^2$ (one-electron transfer) ,

Ti^{4+},

$K^2L^4 \rightarrow K^2L^2$ (two-electron transfer) ,

$K^2L^3 \rightarrow K^2L^2$ (one-electron transfer) .

All of the above processes are consistent with the experimental observations. Moreover, there are no resonances predicted by the calculations that would cause enhancements of any peaks other than K^2L^1 and K^2L^2.

V. CONCLUSIONS

The oxygen $K\alpha$ hypersatellite spectra of a variety of metal oxides have been excited by 2-MeV/amu C and Ar ion impact. Among the spectra excited by C ions, those for CaO, SrO, and CeO_2 exhibited large deviations from binomial distributions caused by certain peaks that appeared to be highly enhanced and others that appeared to be suppressed in intensity. In particular, the following cases were noted: CaO spectrum,

K^2L^1 enhanced, K^2L^2 suppressed,

SrO spectrum,

K^2L^0 enhanced, K^2L^2 suppressed,

CeO_2 spectrum,

K^2L^0 enhanced, K^2L^1 and K^2L^2 suppressed.

The spectral distortions in the above cases are thought to be the result of resonant electron transfer to the highly charged oxygen ion from a neighboring metal ion having energy-matched valence levels.

A method developed previously by Benka et al.[3] for calculating the energy change associated with single-electron transfer (i.e., the resonance energy) was generalized to cover multielectron transfer processes. The contribution of extra-atomic relaxation to the resonance energy was included and found to be significant for the double-K-vacancy states of oxygen. The calculations verified the interpretation of the CaO spectrum in terms of a one-electron transfer to the K^2L^2 vacancy configuration of oxygen and showed that resonant two-electron transfer is a plausible explanation for the distinctive features displayed by the SrO and CeO_2 spectra.

Excitation by Ar ions emphasized the higher-order hypersatellite peaks and enabled a comparison of the spectra according to crystal structure. In general, the spectra for oxides having the same crystal lattice type and comparable ionicities were very similar, and those for oxides not of the same lattice type were distinctly different. However, in spite of the fact that TiO, Ti_2O_3, and TiO_2 belong to different lattice types, their spectra were very similar, and yet they were uniquely different from the spectra obtained for any of the other metal oxides. The greatly enhanced K^2L^1 and K^2L^2 peaks and suppressed K^2L^3, K^2L^4, and K^2L^5 peaks in the spectra of the titanium oxides are indicative of resonant multielectron transfer involving as many as four electrons. Calculations of the resonance condition for various valence states of Ti strongly support this hypothesis.

The model employed in this investigation explicitly assumes that the electrons are transferred in a correlated one-step manner. Correlated two-electron transfer from a target atom to a projectile ion has been observed in low-energy collisions of O^{6+} with He.[28] In this case, the resonance conditions were such that one electron was transferred to the $2p$ level and the other ended up in a Rydberg level having $n \geq 6$.

[1]R. L. Watson, A. K. Keeper, B. I. Sonobe, T. Chiao, and F. E. Jenson, Phys. Rev. A **15**, 914 (1977).

[2]J. A. Demarest and R. L. Watson, Phys. Rev. A **17**, 1302 (1978).

[3]O. Benka, R. L. Watson, and R. A. Kenefick, Phys. Rev. Lett. **47**, 1202 (1981).

[4]O. Benka, R. L. Watson, K. Parthasaradhi, J. M. Sanders, and R. J. Maurer, Phys. Rev. A **27**, 149 (1983).

[5]O. Benka, R. L. Watson, and B. Bandong, Phys. Rev. A **28**, 3334 (1983).

[6]O. Benka, R. L. Watson, B. Bandong, and K. Parthasaradhi, Phys. Rev. A **29**, 123 (1984).

[7]E. Hartmann, J. Phys. B **19**, 1899 (1986).

[8]G. Deconninck and S. Van den Brock, J. Phys. C **13**, 3329 (1980).

[9]O. Benka and M. Uda, Phys. Rev. Lett. **56**, 1667 (1986).

[10]R. L. Watson, B. B. Bandong, J. M. Sanders, and K. Parthasaradhi, Phys. Scr. **31**, 184 (1985).

[11]J. Valjakka, J. Utriainen, T. Aberg, and J. Tulkki, Phys. Rev. B **32**, 6892 (1985).

[12]B. B. Bandong, R. L. Watson, J. Palinkas, and C. Can, J. Phys. B **21**, 1325 (1988).

[13]G. D. Mahan, Phys. Rev. B **21**, 4791 (1980).

[14]G. D. Mahan, Phys. Rev. B **22**, 3102 (1980).

[15]J. A. D. Matthew, M. J. L. Sangster, and C. W. McCambie, J. Phys. C **20**, L205 (1987).

[16]P. H. Citrin and T. D. Thomas, J. Chem. Phys. **57**, 4446 (1972).

[17]R. T. Poole, J. Szajman, R. C. G. Leckey, J. G. Jenkin, and J. Liesegang, Phys. Rev. B **12**, 5872 (1975).

[18]D. Quane, J. Chem. Educ. **47**, 396 (1970).

[19]N. F. Mott and M. J. Littleton, Trans. Farday Soc. **34**, 485 (1938).

[20]G. D. Mahan, Solid State Ionics **1**, 29 (1980).

[21]H. B. Gray, *Electrons and Chemical Bonding* (Benjamin, New York, 1965).

[22]R. W. G. Wyckoff, *Crystal Structures,* 2nd ed. (Interscience, New York, 1963), Vols. I–III.

[23]J. E. Huheey, *Inorganic Chemistry: Principles of Structure and Reactivity,* 2nd ed. (Harper and Row, New York, 1978).

[24]C. E. Moore, *Atomic Energy Levels as Derived from Analyses of Optical Spectra,* Natl. Bur. Stand. (U.S.) Circ. No. 467 (U.S. GPO, Washington, D.C., 1949–1958), Vols. I–III.

[25]J. P. Desclaux, Comput. Phys. Commun. **9**, 31 (1975).

[26]L. A. Grunes, R. D. Leapman, C. N. Wilker, R. Hoffman, and A. B. Kunz, Phys. Rev. B **25**, 7157 (1982).

[27]T. Jo and A. Kotani, Phys. Scr. **35**, 768 (1986).

[28]N. Stolterfoht, C. C. Havener, R. A. Phaneuf, J. K. Swenson, S. M. Shafroth and F. W. Meyer, Phys. Rev. Lett. **57**, 74 (1986).